A paradigmatic system to study the transition from zero/Hopf to double-zero/Hopf bifurcation

Angelo Luongo, Daniele Zulli

▶ **To cite this version:**

Angelo Luongo, Daniele Zulli. A paradigmatic system to study the transition from zero/Hopf to double-zero/Hopf bifurcation. Nonlinear Dynamics, 2012, 70 (1), pp.111-124. hal-00787849

HAL Id: hal-00787849
https://hal.science/hal-00787849

Submitted on 13 Feb 2013

HAL is a multi-disciplinary open access archive for the deposit and dissemination of scientific research documents, whether they are published or not. The documents may come from teaching and research institutions in France or abroad, or from public or private research centers.

L'archive ouverte pluridisciplinaire **HAL**, est destinée au dépôt et à la diffusion de documents scientifiques de niveau recherche, publiés ou non, émanant des établissements d'enseignement et de recherche français ou étrangers, des laboratoires publics ou privés.

A paradigmatic system to study the transition from zero/Hopf to double-zero/Hopf bifurcation

Angelo Luongo · Daniele Zulli

Abstract A two-d.o.f. system experiencing codimension-three double-zero/Hopf bifurcation is considered. This is a special bifurcation which simultaneously involves a defective and a nondefective pair of critical eigenvalues, therefore, requiring a perturbation method specifically tailored on it. A nonstandard version of the multiple scale method is implemented, in which fractional power expansions, both for state-variables and time are used, and high-order arbitrary amplitudes are introduced. Bifurcation equations are obtained, governing the slow flow on the center manifold, which turns out to be tangent to the space spanned by the four critical eigenvectors. These are used to analyze the transition from codimension-three to codimension-two single-zero/Hopf bifurcations, occurring when the modulus of the damping is increased from small to order-one values. Bifurcation charts are obtained, displaying the role of quasi-periodic motions in the transition.

Keywords Multiple scale method · Codimension-3 bifurcation · Double-zero bifurcation · Hopf bifurcation

A. Luongo (✉) · D. Zulli
DISAT, University of L'Aquila, Via Salaria Antica Ovest, 67100 L'Aquila (AQ), Italy
e-mail: angelo.luongo@univaq.it

1 Introduction

Double-zero/Hopf (*DZH*) bifurcation occurs in a dynamical system when, at critical value of the control parameters, the Jacobian matrix admits four non-hyperbolic (central or critical) eigenvalues, two coalescent at zero, and two purely imaginary, namely $\lambda_c = (0, 0, \pm i\omega)$, where i is the imaginary unit. This bifurcation does not seem to have received any attention in the literature, yet probably due to the fact that a codimension-3 bifurcation is believed to be quite rare in practical systems. In spite of this, when a self-excited quasi-Hamiltonian mechanical system is considered, a codimension-2 single-zero/Hopf bifurcation (*ZH*) is likely to occur (see [1]). This is the case, for instance, of structures subject to simultaneous wind and dead loads, leading galloping and buckling phenomena to interact. An example can be found in [2], where a two degree-of-freedom rigid rod is excited by an axial load and a transverse flow, giving rise to a codimension-two zero-Hopf bifurcation. However, several other examples, picked up from paradigmatic models as well as actual engineering problems, are given in [3–13]. In this kind of bifurcation, the critical eigenvalues of the Jacobian matrix are $\lambda_c = (0, \pm i\omega)$; if, however, the damping ξ is small, a fourth stable eigenvalue $\lambda_s = -\xi < 0$ is close to the imaginary axis, thus leaving ambiguous how to tackle this bifurcation, namely if it is a *ZH* or, in contrast, a perturbation of a *DZH*-bifurcation. The two dynamics are expected to be quite different, since according to the cen-

ter manifold theory, the former one occurs on a three-dimensional variety of the state-space, while the latter one occurs on a four-dimensional variety. It is conjectured that a transition should exist between the two regimes, when the damping coefficient is quasistatically varied, which is worth studying here. In general, the study of abrupt or smooth transition phenomena in dynamics is a very challenging issue (see [14–16]). Often, a suitable way to study transitions is starting from the most complex system, then descending to the easier one by smooth modification of a significant parameter. This is the strategy adopted herein.

As it has been widely discussed in previous works, the multiple scale method (MSM) [17–19] appears to be one of the most efficient tool to tackle bifurcation problems. As a matter of fact, it reduces the system to its essential dimension, as the center manifold method does, by accounting both for active and passive variables, and *simultaneously* it selects the essentially nonlinear terms, as the normal form theory does. In addition, the MSM furnishes amplitude-equations for the slow-flow, in which the fast dynamics have been filtered. In spite of this, neither the MSM nor other perturbation methods seem to be available to tackle a "difficult" bifurcation, in which a defective (not semisimple) double-zero eigenvalue interacts with a non-defective pair of Hopf eigenvalues. Hence, a specific algorithm must be tailored on the problem.

Here, a nonstandard version of the multiple scales method is implemented to get the bifurcation equations for a system experiencing double-zero/Hopf bifurcation. This technique has been already used in [20], where a nonautonomous system has been considered, in a specific resonance condition and under ad hoc assumptions. Herein, however, the method is proposed for an autonomous system, in a systematic version, in principle able to be carried out at any perturbation order.

The algorithm is illustrated referring to a 2 d.o.f. "paradigmatic system", which is representative of a large class of mechanical systems, exhibiting such a kind of bifurcation. It consists of two oscillators, weakly coupled by nonlinear viscous-elastic devices. One of them undergoes Hopf bifurcation caused, for example, by aerodynamic forces vanishing its structural damping; the other one suffers a double-zero bifurcation due, for example, to a gravitational load which zeroes its linear stiffness, and to an evanescently small structural damping.

Attention is focused on the transition from the codimension-3 *DZH*-bifurcation to codimension-2 *ZH*-bifurcation, allowing the damping to become large in modulus. Actually, this is only one of the possible transitions from a *DZH*-bifurcation, leaving to future works the analysis of other paths as well as the complete unfolding of the neighborhood of the bifurcation point. Preliminary results have been presented in [21]. The paper is organized as follows. In Sect. 2, a two-d.o.f. mechanical model is considered, in Sect. 3, the MSM is implemented, in Sect. 4, the transition from *DZH*- to *ZH*-bifurcations is qualitatively described, in Sect. 5 numerical results are shown, and in Sect. 6 some conclusions are drawn.

2 The model

A paradigmatic autonomous system is considered (see Fig. 1), made of two oscillators of mass m_1 and m_2, respectively, linked each other and to the ground by cubic elastic springs and Van Der Pol dampers. It represents a class of coupled Duffing–Van Der Pol oscillators (see [22–28]). The linear coefficients of the springs and of the dashpots are denoted by k_{i1} and c_{i1}, respectively, and their cubic coefficients by k_{i3} and c_{i3} ($i = 0, 1, 2$). Displacements of the masses from their rest positions are denoted by $x(t)$ and $y(t)$, respectively, t being the time.

Physical systems falling in this class are structures under wind flow, causing Hopf bifurcation, and dead loads, causing elastic buckling. Accordingly, the coefficients of the linear terms, c_{11} (accounting for structural and aerodynamic damping) and k_{21} (accounting for elastic and geometric stiffness) are allowed to vanish and to become negative, when the relevant destabilizing effects prevail on the stabilizing ones. Similarly, the damping coefficient c_{21} is assumed to be positive, ranging from small to very small values, in order to span the transition region.

The natural frequencies of the oscillators, when damping and coupling are removed, are $\omega_1 =$

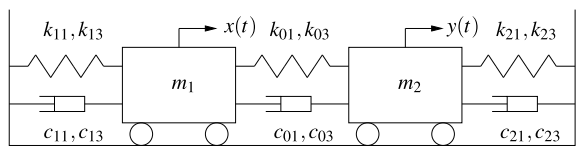

Fig. 1 Scheme of the two oscillators

$\sqrt{k_{11}/m_1}$ and $\omega_2 = \sqrt{k_{21}/m_2}$, respectively. Nondimensional quantities are introduced:

$$t^* = \omega_1 t, \qquad x^* = \frac{x}{\ell}, \qquad y^* = \frac{y}{\ell}, \tag{1}$$

where ℓ is a characteristic length, and

$$\begin{aligned}
&\mu = -\frac{c_{11}}{m_1\omega_1^2}, \quad \xi = -\frac{c_{21}}{m_2\omega_1},\\
&\nu = -\frac{\omega_2^2}{\omega_1^2}, \quad \kappa_{13} = \frac{k_{13}\ell^2}{m_1\omega_1^2},\\
&\xi_{13} = \frac{c_{13}\ell^2}{m_1\omega_1}, \quad \kappa_{03} = \frac{k_{03}\ell^2}{m_1\omega_1^2},\\
&\xi_{03} = \frac{c_{03}\ell^2}{m_1\omega_1}, \quad \kappa_{01} = \frac{k_{01}}{m_1\omega_1^2},\\
&\xi_{01} = \frac{c_{01}}{m_1\omega_1}, \quad \alpha = \frac{m_1}{m_2},\\
&\kappa_{23} = \frac{k_{23}\ell^2}{m_2\omega_1^2}, \quad \xi_{23} = \frac{c_{23}\ell^2}{m_2\omega_1}.
\end{aligned} \tag{2}$$

Dropping the asterisks, the equations of motions

$$\begin{aligned}
&\ddot{x} - \mu\dot{x} + x + \kappa_{13}x^3 + \xi_{13}\dot{x}x^2 - \kappa_{01}(y-x)\\
&\quad - \kappa_{03}(y-x)^3 - \xi_{01}(\dot{y}-\dot{x})\\
&\quad - \xi_{03}(\dot{y}-\dot{x})(y-x)^2 = 0,
\end{aligned} \tag{3a}$$

$$\begin{aligned}
&\ddot{y} - \xi\dot{y} - \nu y + \kappa_{23}y^3 + \xi_{23}\dot{y}y^2 + \alpha\kappa_{01}(y-x)\\
&\quad + \alpha\kappa_{03}(y-x)^3 + \alpha\xi_{01}(\dot{y}-\dot{x})\\
&\quad + \alpha\xi_{03}(\dot{y}-\dot{x})(y-x)^2 = 0
\end{aligned} \tag{3b}$$

where the dot indicates differentiation with respect to the nondimensional time.

The parameters μ, ν, ξ in Eqs. (3a) and (3b), as well as the linear coupling terms κ_{01}, ξ_{01} are assumed to be small. This means that the real system is close to an ideal uncoupled system simultaneously experiencing: (a) a Hopf bifurcation (H) triggering the x-oscillator (since its linear damping is vanishing), and (b) a double-zero bifurcation (DZ) triggering the y-oscillator (since its linear damping and stiffness are both vanishing). Definitions in Eq. (2) for the parameters μ, ν entail that, when they are negative, the trivial equilibrium is stable, while zero-values denotes incipient bifurcations. For example, when $\nu < 0$, the y-oscillator has positive linear stiffness (see Eq. (3b)); on the other hand, when $\nu > 0$, the y-oscillator has a negative stiffness and, consequently, no real frequency. Analogous considerations can be made for μ. Accordingly, μ, ν, ξ are assumed as bifurcation parameters, so that the origin of the (μ, ν, ξ)-parameter space is a *DZH* codimension-3 bifurcation point. The small elastic and viscous coupling of course slightly modifies the position of the bifurcation in the parameter space, but they are considered as fixed, auxiliary parameters.

It is important to observe that the two masses m_1 and m_2 are considered here to be of the same order (differently, e.g., from similar systems studied in the context of nonlinear energy sinks; see [29]); consequently, the mass ratio α is of order 1.

3 Multiple Scale analysis

3.1 Bifurcation equations

Equations (3a) and (3b) are analyzed by the multiple scale method. A dimensionless small parameter ε is introduced to rescale the equations. The dependent variables (x, y) and the coefficients are ordered as follows: $(x, y) = \varepsilon^{1/2}(\hat{x}, \hat{y})$; $(\mu, \nu, \xi, \kappa_{01}, \xi_{01}) = \varepsilon(\hat{\mu}, \hat{\nu}, \hat{\xi}, \hat{\kappa}_{01}, \hat{\xi}_{01})$, so that Eqs. (3) become (omitting the hats)

$$\begin{aligned}
&\ddot{x} + x + \varepsilon\big[-\mu\dot{x} + \kappa_{13}x^3 + \xi_{13}\dot{x}x^2\\
&\quad - \kappa_{01}(y-x) - \kappa_{03}(y-x)^3\\
&\quad - \xi_{01}(\dot{y}-\dot{x}) - \xi_{03}(\dot{y}-\dot{x})(y-x)^2\big] = 0,\\
&\ddot{y} + \varepsilon\big[-\xi\dot{y} - \nu y + \kappa_{23}y^3 + \xi_{23}\dot{y}y^2\\
&\quad + \alpha\kappa_{01}(y-x) + \alpha\kappa_{03}(y-x)^3\\
&\quad + \alpha\xi_{01}(\dot{y}-\dot{x}) + \alpha\xi_{03}(\dot{y}-\dot{x})(y-x)^2\big] = 0.
\end{aligned} \tag{4}$$

The bifurcation under analysis is triggered by the occurrence of a double-zero eigenvalue, associated with a Jordan block of the (nilpotent) Jacobian matrix. Such a kind of eigenvalue is said "defective," since an incomplete set of (proper) eigenvectors is associated with it, so that generalized eigenvectors must be evaluated to complete the basis. As it has been shown in literature, by dealing with linear algebraic problems [30, 31] and nonlinear dynamical systems [18, 32, 33], standard perturbation methods, based on integer power series expansions of the perturbation parameter, fail, essentially due to the fact that the proper eigenvectors belong to the range of the operator, so that

resonant terms, which are external to the range, cannot be removed. Hence, fractional power series expansions must be used, permitting the appearance of generalized eigenvectors at the intermediate steps; among them, the eigenvector of highest index has nonzero projection out of the range of the operator and, therefore, it is able to remove the resonant term.

However, the problem here dealt with, possesses a specific aspect from an algorithmic point of view, which to the authors' knowledge, has not been analyzed yet, namely that a subset of the eigenvalues (the double zero) is defective, and the remaining subset in nondefective (the simple $\pm i$ eigenvalues). Therefore, while the first eigenvalues call for a fractional series expansion, the other two would require integer powers. Here, we will show that fractional powers also work but, as expected, trivial information are got at some perturbation orders, as a consequence of the mixed nature of the critical eigenvalues.

Accordingly, the dependent variables in Eq. (4) are expanded as

$$\begin{Bmatrix} x \\ y \end{Bmatrix} = \begin{Bmatrix} x_0 \\ y_0 \end{Bmatrix} + \varepsilon^{1/2} \begin{Bmatrix} x_1 \\ y_1 \end{Bmatrix} + \varepsilon \begin{Bmatrix} x_2 \\ y_2 \end{Bmatrix} + \cdots \tag{5}$$

and independent time scales $t_0 := t$, $t_1 := \varepsilon^{1/2} t$, $t_2 := \varepsilon t, \ldots$, are introduced. Therefore, the derivatives with respect to the time assume the expressions

$$\begin{aligned} \frac{d}{dt} &= d_0 + \varepsilon^{1/2} d_1 + \varepsilon d_2 + \cdots, \\ \frac{d^2}{dt^2} &= d_0^2 + 2\varepsilon^{1/2} d_0 d_1 + \varepsilon \left(d_1^2 + 2 d_0 d_2 \right) + \cdots, \\ d_i &:= \frac{\partial}{\partial t_i}. \end{aligned} \tag{6}$$

The perturbation equations therefore read:

$\mathcal{O}\left(\varepsilon^0\right)$:

$$\begin{aligned} d_0^2 x_0 + x_0 &= 0, \\ d_0^2 y_0 &= 0, \end{aligned} \tag{7}$$

$\mathcal{O}\left(\varepsilon^{1/2}\right)$:

$$\begin{aligned} d_0^2 x_1 + x_1 &= -2 d_0 d_1 x_0, \\ d_0^2 y_1 &= -2 d_0 d_1 y_0, \end{aligned} \tag{8}$$

$\mathcal{O}\left(\varepsilon^1\right)$:

$$\begin{aligned} d_0^2 x_2 + x_2 &= \mathcal{F}_2(x_0, y_0, x_1), \\ d_0^2 y_2 &= \mathcal{G}_2(x_0, y_0, y_1), \end{aligned} \tag{9}$$

$\mathcal{O}\left(\varepsilon^{3/2}\right)$:

$$\begin{aligned} d_0^2 x_3 + x_3 &= \mathcal{F}_3(x_0, y_0, x_1, y_1, x_2), \\ d_0^2 y_3 &= \mathcal{G}_3(x_0, y_0, x_1, y_1, y_2) \end{aligned} \tag{10}$$

where $\mathcal{F}_i, \mathcal{G}_i$, $(i = 2, 3)$ are given in Appendix B. Equations of order $\mathcal{O}(\varepsilon^2)$, although used, are not shown here for sake of brevity.

The generating equation (7) admits the following not-diverging solution:

$$\begin{Bmatrix} x_0 \\ y_0 \end{Bmatrix} = \begin{Bmatrix} A_0(t_1, \ldots) \exp(i t_0) + cc \\ B_0(t_1, \ldots) \end{Bmatrix} \tag{11}$$

where cc denotes the complex conjugate, A_0 is a complex amplitude, and B_0 a real amplitude; both unknown quantities, slowly depending on time.

As usual, the algorithm calls for recursively solving the perturbation equations and removing resonant terms in their right-hand members, namely frequency-1 harmonics in the upper equations, and frequency-0 harmonics in the lower equations. After removing resonant terms, the solution to the $\varepsilon^{k/2}$-order reads as

$$\begin{Bmatrix} x_k \\ y_k \end{Bmatrix} = \begin{Bmatrix} x_k^*(t_0, t_1, \ldots) + A_k(t_1, \ldots) \exp(i t_0) + cc \\ y_k^*(t_0, t_1, \ldots) + B_k(t_1, \ldots) \end{Bmatrix}, \quad k = 1, 2, \ldots \tag{12}$$

where $x_k^*(t_0, t_1, \ldots)$, $y_k^*(t_0, t_1, \ldots)$ are particular solutions, and $A_k(t_1, \ldots)$, $B_k(t_1, \ldots)$ are arbitrary amplitudes appearing in the complementary part of the solution. These latter quantities are usually omitted in literature, or merely used for normalization purposes [34], since they repeat the generating solution, and they can be reabsorbed in "total amplitudes A and B" at the end of the procedure [17]. However, as it will be shown ahead, the standard approach fails in the case under study, since some inconsistencies appear in the procedure, and reconstitution cannot be performed. To overcome the drawback, the arbitrary amplitudes A_k, B_k were systematically introduced at each orders, leading to correctly reconstituted bifurcation equations. Unfortunately, all the intermediate steps required cumbersome algebra, suggesting the tentative omission of part of the amplitudes. It was found that the amplitude A_1, appearing at the $\varepsilon^{1/2}$-order, is the only one which needs to be introduced, since it leads to results which

are identical to those of the complete procedure. An explanation of this circumstance will be given below.

After substitution of Eq. (11) in the perturbation equation of order $\varepsilon^{1/2}$ (Eqs. (8)), a resonant term (of frequency 1) appears in the first equation, while no resonant terms (of frequency 0) appear in the second equation. The vanishing of the resonant term furnishes

$$d_1 A_0 = 0. \tag{13}$$

Since $x_0^* = 0$, $y_0^* = 0$, and according to the previous discussion, solution to Eqs. (8) is taken as

$$\begin{Bmatrix} x_1 \\ y_1 \end{Bmatrix} = \begin{Bmatrix} A_1(t_1, \ldots)\exp(it_0) + cc \\ 0 \end{Bmatrix}. \tag{14}$$

Then removal of resonant terms from Eqs. (9) leads to

$$d_2 A_0 + d_1 A_1 = \alpha_1 A_0 + \alpha_2 A_0 B_0^2 + \alpha_3 A_0^2 \bar{A}_0, \tag{15a}$$

$$d_1^2 B_0 = \beta_1 B_0 + \beta_2 B_0^3 + \beta_3 A_0 \bar{A}_0 B_0 \tag{15b}$$

where the overbar denotes complex conjugate and the coefficients α_i and β_i are reported in Appendix B. Going on to the higher orders and systematically taking

$$\begin{Bmatrix} x_k \\ y_k \end{Bmatrix} = \begin{Bmatrix} x_k^*(t_0, t_1, \ldots) + cc \\ y_k^*(t_0, t_1, \ldots) + cc \end{Bmatrix}, \quad k = 2, 3, \ldots \tag{16}$$

with x_k^*, y_k^* here omitted for brevity, the following solvability condition is found at the $\varepsilon^{3/2}$-order:

$$\begin{aligned} &d_3 A_0 + d_2 A_1 \\ &\quad = \alpha_1 A_1 + \alpha_2 A_1 B_0^2 + \alpha_3\big(2A_0\bar{A}_0 A_1 + A_0^2 \bar{A}_1\big) \\ &\qquad + \alpha_4 A_0 B_0 d_1 B_0 + \alpha_5 d_1^2 A_1, \end{aligned} \tag{17a}$$

$$\begin{aligned} 2d_1 d_2 B_0 &= \beta_3(A_1\bar{A}_0 + A_0\bar{A}_1)B_0 \\ &\quad + \big(\beta_4 + \beta_5 B_0^2 + \beta_6 A_0\bar{A}_0\big)d_1 B_0 \end{aligned} \tag{17b}$$

and the following one at the ε^2-order

$$\begin{aligned} &d_4 A_0 + d_3 A_1 \\ &\quad = \alpha_1 A_2 + \alpha_3\big(A_1^2\bar{A}_0 + 2A_0 A_1 \bar{A}_1\big) \\ &\qquad + \alpha_4(A_1 B_0 d_1 B_0 + A_0 B_0 d_2 B_0) \\ &\qquad + \alpha_5\big(d_2^2 A_0 + 2d_1 d_2 A_1\big) \\ &\qquad + \alpha_6(d_1 A_1 + d_2 A_0) \\ &\qquad + \alpha_7\big(A_0^2(d_1\bar{A}_1 + d_2\bar{A}_0) \\ &\qquad + A_0\bar{A}_0(d_1 A_1 + d_2 A_0)\big) \\ &\qquad + \alpha_8 B_0^2(d_1 A_1 + d_2 A_0) + \alpha_9 A_0 \\ &\qquad + \alpha_{10} A_0 B_0^2 + \alpha_{11} A_0^2 \bar{A}_0, \end{aligned} \tag{18}$$

$$\begin{aligned} &d_2^2 B_0 + 2d_1 d_3 B_0 \\ &\quad = \beta_3(A_2\bar{A}_0 B_0 + A_1\bar{A}_1 B_0 + A_0\bar{A}_2 B_0) \\ &\qquad + \beta_4 d_2 B_0 + \beta_5 B_0^2 d_2 B_0 \\ &\qquad + \beta_6(A_0\bar{A}_0 d_2 B_0 + A_1\bar{A}_0 d_1 B_0 \\ &\qquad + A_0\bar{A}_1 d_1 B_0) + \beta_7\big(A_0 B_0(d_1\bar{A}_1 + d_2\bar{A}_0) \\ &\qquad + \bar{A}_0 B_0(d_1 A_1 + d_2 A_0)\big) + \beta_8 B_0 + \beta_9 B_0^3 \\ &\qquad + \beta_{10} A_0\bar{A}_0 B_0. \end{aligned}$$

The need for introducing the arbitrary amplitude A_1 is now discussed. Because of Eq. (13), the right-hand side of Eq. (15a) contains terms generally depending on the time-scale t_1 (through B_0) and terms independent of this scale (pure terms in A_0). If Eq. (15a) is differentiated with respect to t_1, and use is made of Eq. (13), it follows:

$$d_1^2 A_1 = 2\alpha_2 A_0 B_0 d_1 B_0. \tag{19}$$

If A_1 were not introduced ($A_1 \equiv 0$ in Eq. (19)), it would turn out $d_1 B_0 \equiv 0$, inconsistently with Eq. (15b) which states that, in general, $d_1^2 B_0 \neq 0$. Such an inconsistency, however, does not occur at higher orders and, therefore, additional arbitrary amplitudes are not strictly necessary.

The reconstitution procedure must now be applied to get the Amplitude Modulation Equations (AME). Accordingly, the total amplitudes $A = A_0 + \varepsilon^{1/2} A_1$ and $B = B_0$ and their time derivatives are introduced, written as:

$$\begin{aligned} \dot{A} &= \varepsilon(d_2 A_0 + d_1 A_1) + \varepsilon^{3/2}(d_3 A_0 + d_2 A_1) \\ &\quad + \varepsilon^2(d_4 A_0 + d_3 A_1), \end{aligned} \tag{20a}$$

$$\begin{aligned} \ddot{B} &= \varepsilon d_1^2 B_0 + 2\varepsilon^{3/2} d_1 d_2 B_0 \\ &\quad + \varepsilon^2\big(d_2^2 B_0 + 2d_1 d_3 B_0\big). \end{aligned} \tag{20b}$$

Moreover the inverse rescaling $\varepsilon(\mu, \nu, \xi, \kappa_{01}, \xi_{01}) \to (\mu, \nu, \xi, \kappa_{01}, \xi_{01})$, $\varepsilon^{3/2}(A, B) \to (A, B)$ must be used to come back to the original variables.

It appears from Eqs. (20a) and (20b) that the time-derivative operator d/dt is of order ε when it acts on A, while it is of order $\varepsilon^{1/2}$ when it acts on B, as a

consequence of $d_1 A_1 = 0$ (Eq. (13)). It entails that B is more rapidly varying than A. These results will be used ahead.

As usual in the standard MSM, the right-hand side of Eqs. (20a) and (20b) must be transformed by properly making use of the solvability conditions at different orders. The aim is to obtain derivatives of the amplitudes reconstituted on the true time scale t, consistently with the maximum order retained in the analysis. Here, however, due to the fact that arbitrary amplitudes were introduced at each steps, the reconstitution procedure is not straightforward and it requires some strategies to be pursued. Indeed, substitution of Eqs. (13), (15a), (15b), (17a), (17b), (18) in the right-hand side of Eq. (20a) leads the occurrence, at different orders, of several terms generally classifiable in three different categories: (a) terms of type $d_2 A_0 + d_1 A_1$, that can be directly tackled by using the solvability condition (15a); (b) terms of type $d_1^2 A_1$, that, as in the standard version of the MSM, can be tackled by t_1-differentiating the solvability condition (15a) (getting to Eq. (19)); (c) terms of type $d_2^2 A_0 + 2 d_1 d_2 A_1$, which call for a special treatment (discussed in Appendix A), as a consequence of the fact that they involve the addition of second derivatives of amplitudes of different order.

The procedure leads to the following reconstituted equations in the true (nondimensional) time:

$$\begin{aligned}\dot{A} &= \left[\gamma_1 + \mu\gamma_2 + \mu^2\gamma_3\right]A + \left[\gamma_4 + \mu\gamma_5\right]A^2\bar{A} \\ &\quad + \gamma_6 A\dot{B}^2 + \gamma_7 AB\dot{B} \\ &\quad + \left[\gamma_8 + \nu\gamma_9 + \mu\gamma_{10}\right]AB^2, \end{aligned} \tag{21a}$$

$$\begin{aligned}\ddot{B} &+ \left(\xi + \eta_{11} + \eta_{12}A\bar{A} + \eta_{13}B^2\right)\dot{B} \\ &+ \left[\nu + \eta_{14} + (\eta_{15} + \mu\eta_{16})A\bar{A}\right]B \\ &+ \eta_{17}B^3 = 0 \end{aligned} \tag{21b}$$

where $\gamma_i = \eta_i + i\zeta_i$ $(i = 1, \ldots, 10)$, $\eta_i \in \mathbb{R}$ $(i = 11, \ldots, 17)$ are reported in Appendix B. It is worth noticing that if the arbitrary amplitude A_1 were not introduced, the term $\gamma_7 AB\dot{B}$ in Eq. (21a) would not have appeared.

The polar form of Eqs. (21a) and (21b), obtained posing $A := \frac{1}{2}ae^{i\vartheta}$ (and referred as polar amplitude modulation equations), is:

$$\begin{aligned}\dot{a} &= \left(\eta_1 + \mu\eta_2 + \mu^2\eta_3\right)a + \frac{1}{4}(\eta_4 + \mu\eta_5)a^3 \\ &\quad + \eta_6 aB^2 + \eta_7 aB\dot{B} \\ &\quad + (\eta_8 + \nu\eta_9 + \mu\eta_{10})a\dot{B}^2, \end{aligned} \tag{22a}$$

$$\begin{aligned}\ddot{B} &+ \left(\xi + \eta_{11} + \frac{\eta_{12}}{4}a^2 + \eta_{13}B^2\right)\dot{B} \\ &+ \left[\nu + \eta_{14} + \frac{1}{4}(\eta_{15} + \mu\eta_{16})a^2\right]B \\ &+ \eta_{17}B^3 = 0, \end{aligned} \tag{22b}$$

$$\begin{aligned}a\dot{\vartheta} &= \left(\zeta_1 + \mu\zeta_2 + \mu^2\zeta_3\right)a + \frac{1}{4}(\zeta_4 + \mu\zeta_5)a^3 \\ &\quad + \zeta_6 aB^2 + \zeta_7 aB\dot{B} \\ &\quad + (\zeta_8 + \nu\zeta_9 + \mu\zeta_{10})a\dot{B}^2. \end{aligned} \tag{22c}$$

Equations (22a), (22b) and (22c) are the normal form of the bifurcation equations for the *DZH* bifurcation; they are believed to be new.

In Eqs. (22a), (22b) and (22c) the variable ϑ is a slave of a, B; therefore, Eq. (22c) can be solved, in principle, once a, B have been obtained from Eqs. (22a) and (22b).

3.2 Fixed points analysis

The fixed points of Eqs. (22a), (22b) and (22c) are obtained by letting $a = a_e = \text{const}$, $B = B_e = \text{const}$. Since ξ appears only as a coefficient of $\dot{B}$, it means that the fixed points are independent of ξ, which is involved only in the stability analysis.

The trivial solution $a_e = B_e = 0$, indicated as 0, exists for any values of the parameters. Two different monomodal solutions are also found: the first one, indicated as I, is:

$$\begin{aligned} a_e &= 2\sqrt{\frac{2\mu}{3\mu(\kappa_{03} + \kappa_{13}) + 2(\xi_{03} + \xi_{13})}}, \\ B_e &= 0. \end{aligned} \tag{23}$$

In terms of the original variables, it describes a periodic motion in $x(t)$, while $y(t)$ is of higher order. The second one, indicated as II, is:

$$\begin{aligned} a_e &= 0, \\ B_e &= \sqrt{\frac{\nu}{\alpha\kappa_{03} + \kappa_{23}}} \end{aligned} \tag{24}$$

which describes a static deflection (buckling) in the y-coordinate, while x is of higher order. A bimodal

solution is also found, indicated as III, of kind

$$\begin{aligned} a_e &= a(\mu, \nu), \\ B_e &= B(\mu, \nu) \end{aligned} \tag{25}$$

representing periodic oscillations of the variable $x(t)$, when $y(t)$ is statically deflected. The full analytical expression of the solution III is not reported since it is very cumbersome. The stability of all the solutions is ruled by the real part of the eigenvalues of the Jacobian matrix of Eqs. (22a) and (22b).

In addition to equilibria and periodic motions, quasi-periodic motions (QP) do exist, in which $A(t + T) = A(t)$, $B(t + T) = B(t)$ are periodic of period T; this entailing that $x(t)$ is biperiodic of periods 2π and T, while $y(t)$ is periodic of period T. Such solutions have been numerically found by direct integrations of Eqs. (22a), (22b) and (22c) and a continuation method [35].

4 Transition from *DZH*- to *ZH*-bifurcation

An exhaustive analysis of the bifurcation equations in the three-dimensional parameter space is a difficult task, which is left for future investigations. Here, a simpler analysis is carried out, aimed to highlight the mechanism of transition from codimension-3 to codimension-2 bifurcations (Fig. 2). To this end, a planar analysis is performed, in which one of the three parameters is kept constant, and the analysis is repeated for increasing (in modulus) values of the parameter, from small to $\mathcal{O}(1)$ values (although this entails an ordering violation in the bifurcation equations). As an expected result, the bifurcation equations should describe the lowering of the codimension of the bifurcation.

For example, if planes $\xi = \text{const} < 0$ are considered, with $|\xi| = \mathcal{O}(1)$, the typical scenario of the *ZH*-bifurcation occurs (Fig. 2). Indeed, on this plane, one of the four critical eigenvalues involved in *DZH*-bifurcation is far enough from the imaginary axis, so that it passively contributes to the motion on the center manifold. Similarly, planes $\mu = \text{const} < 0$, $|\mu| = \mathcal{O}(1)$ and $\nu = \text{const} < 0$, $|\nu| = \mathcal{O}(1)$ represent the scenarios of *DZ*- and *DH*-bifurcations, respectively. Here, attention is limited to the transition from *DZH*- to *ZH*-bifurcations.

The bifurcation equations (21a) and (21b) are considered again, and the order of magnitude of all their

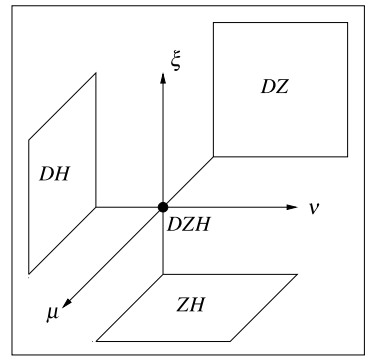

Fig. 2 Scheme of transitions

terms is evaluated. Since the bifurcation parameters are all $\mathcal{O}(\varepsilon)$, the amplitudes A and B are $\mathcal{O}(\varepsilon^{1/2})$ and their time derivatives (as previously observed) are $(d/dt)A = \mathcal{O}(\varepsilon \times \varepsilon^{1/2})$, $(d/dt)B = \mathcal{O}(\varepsilon^{1/2} \times \varepsilon^{1/2})$; Eqs. (21a) and (21b) have the following structure:

$$\begin{cases} \underbrace{\dot{A}}_{\varepsilon^{3/2}} = \mathcal{L}_1(\underbrace{\mu A, A^2\bar{A}, AB^2}_{\varepsilon^{3/2}}; \underbrace{A\dot{B}\bar{B}}_{\varepsilon^2}; \underbrace{A\dot{B}^2}_{\varepsilon^{5/2}}), \\ \underbrace{\ddot{B}}_{\varepsilon^{3/2}} = \mathcal{L}_2(\underbrace{\nu B, B^3, A\bar{A}B}_{\varepsilon^{3/2}}; \underbrace{\xi\dot{B}}_{\varepsilon^2}; \underbrace{B^2\dot{B}, A\bar{A}\dot{B}}_{\varepsilon^{5/2}}) \end{cases} \tag{26}$$

where $\mathcal{L}$ are linear operators, and the order of magnitude of all the terms is reported below them.

When $\xi \to \mathcal{O}(1)$, the bifurcation turns out to be non-defective, and fractional time scales are not involved. Therefore, it is still $(d/dt)A = \mathcal{O}(\varepsilon \times \varepsilon^{1/2})$, but $(d/dt)B = \mathcal{O}(\varepsilon \times \varepsilon^{1/2})$, entailing that $\ddot{B}$ switches to a higher order. This means that as $|\xi|$ is increased, the dynamics of the variable B becomes slower. Consequently, at the leading order, Eqs. (21a) and (21b) tend to:

$$\begin{cases} \dot{A} = \dfrac{\mu}{2}A + \kappa_1 A^2\bar{A} + \kappa_2 AB^2, \\ \dot{B} = -\dfrac{\nu}{\xi}B - \dfrac{\kappa_3}{\xi}A\bar{A}B + \dfrac{\kappa_4}{\xi}B^3 \end{cases} \tag{27}$$

which are, indeed, the equations governing *ZH*-bifurcation [2]. It is worth noticing that, since $A \in \mathbb{C}$ and $B \in \mathbb{R}$, Eqs. (26) are a four-dimensional dynamical system, while Eqs. (27) are a three-dimensional system. This occurrence is consistent with the fact that one of the four central eigenvalues becomes stable in the limit process. Moreover, since the phase of A is a slave variable for both Eqs. (26) and Eqs. (27), the essential dynamics are captured by a system whose dimension, 3 or 2, equates the codimension of the bifurcation.

As a conclusion of the limit analysis, the bifurcation equations (21a) and (21b) for *DZH* correctly tend to that for *ZH*; therefore, they can be used for small to large values (in modulus) of the damping parameter ξ. In contrast, of course, Eqs. (27) do not tend to Eqs. (26), when $\xi \to 0$.

5 Numerical results

The following numerical values are used for the auxiliary parameters: $\alpha = 2.2$, $\kappa_{01} = 0$, $\xi_{01} = 0$, $\kappa_{03} = 1.8$, $\xi_{03} = -1.0$, $\kappa_{13} = 10.0$, $\xi_{13} = 8.0$, $\kappa_{23} = -1.0$, $\xi_{23} = 1.0$. Since both κ_{01} and ξ_{01} are assumed as zero in the numerical evaluations, no actual shift of the *DZH* bifurcation point occurs from the origin of the (μ, ν, ξ)-space. The transition phenomenon is described in the next Figs. 3, 4, 9, where the bifurcation loci of the nontrivial solutions of Eqs. (22a), (22b) and (22c) are shown in the (μ, ν)-plane. Different values of ξ are considered, starting from values close to the *DZH*-bifurcation (small $|\xi|$) and then moving away toward a *ZH*-bifurcation (large $|\xi|$). Bifurcation diagrams showing the amplitudes a and B vs. the bifurcation parameter μ are also plotted; they can be viewed as planar sections of three-dimensional bifurcation diagrams in the (μ, ν, a)- and (μ, ν, B)-spaces.

A small value of damping $\xi = -0.05$ is considered first (Fig. 3). In Fig. 3a the shadow indicates the stable region of the trivial solution 0 (both μ and ν negative); the blue line indicates the loci of bifurcation where a supercritical branch I emanates from (see Fig. 3b and 3c); the green line indicates the loci of bifurcation where a supercritical branch II emanates from (see Fig. 3c); the red lines are the boundaries of the region where the solution III exists (see Fig. 3b and 3c). Moreover, lines related to successive bifurcations (i.e., not from the trivial solution), causing stable (black, QP1) and unstable (magenta, QP2 and QP3) quasiperiodic oscillations, are reported.

Figures 3b and 3c show the amplitudes a, B vs. μ when $\xi = -0.05$, $\nu = 0.1$. It appears that the purely buckled solution in y (solution II, green) exists for negative μ, when x is of higher order ($a = 0, B \neq 0$). Increasing the values of μ, a periodic motion in x arises when the system is buckled in the y-coordinate (solution III, red). This motion becomes unstable and a quasiperiodic one starts (QP1, black), where both a and B are periodic. Further increasing μ, the quasiperiodic motion QP1 dies, and after a while, a periodic motion in x becomes stable when y is of higher order (solution I, blue). An unstable quasiperiodic motion (QP3, magenta) coexists with the other solutions in the interval $\mu \in [-0.075, 0.1]$. Superimposed with the results from the MSM, results from numerical integrations are also shown in Figs. 3b and 3c (colored boxes, just for stable branches) in good agreement.

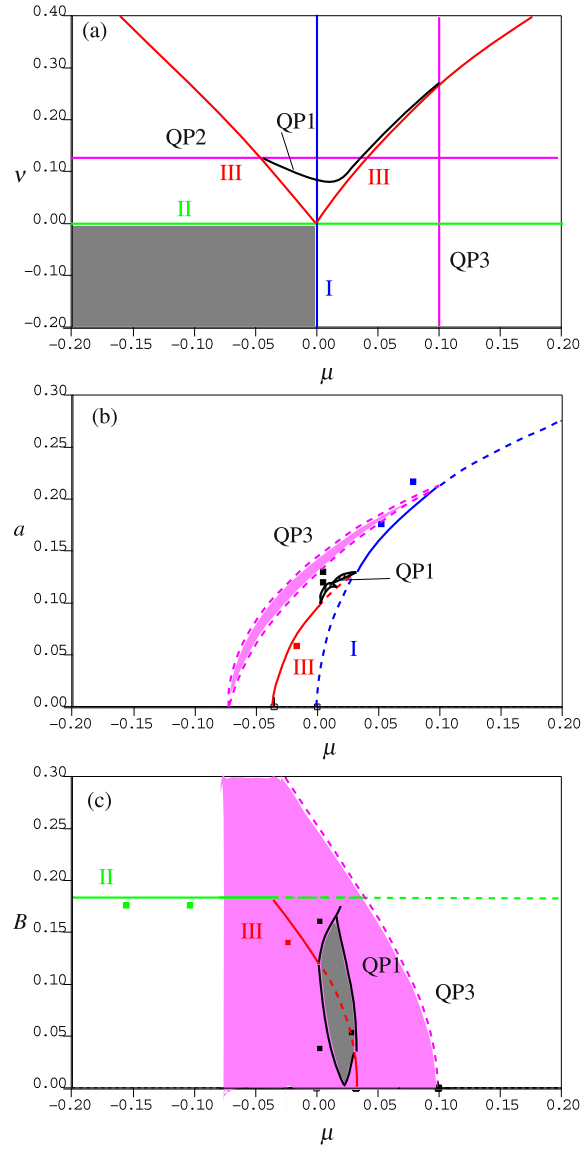

Fig. 3 Bifurcation diagrams when $\xi = -0.05$; (**a**) bifurcation loci on the (μ, ν)-plane; (**b**, **c**): amplitudes a and B vs. μ when $\xi = -0.05$ and $\nu = 0.1$. *Continuous line*: stable; *dashed line*: unstable; *boxes*: direct integrations

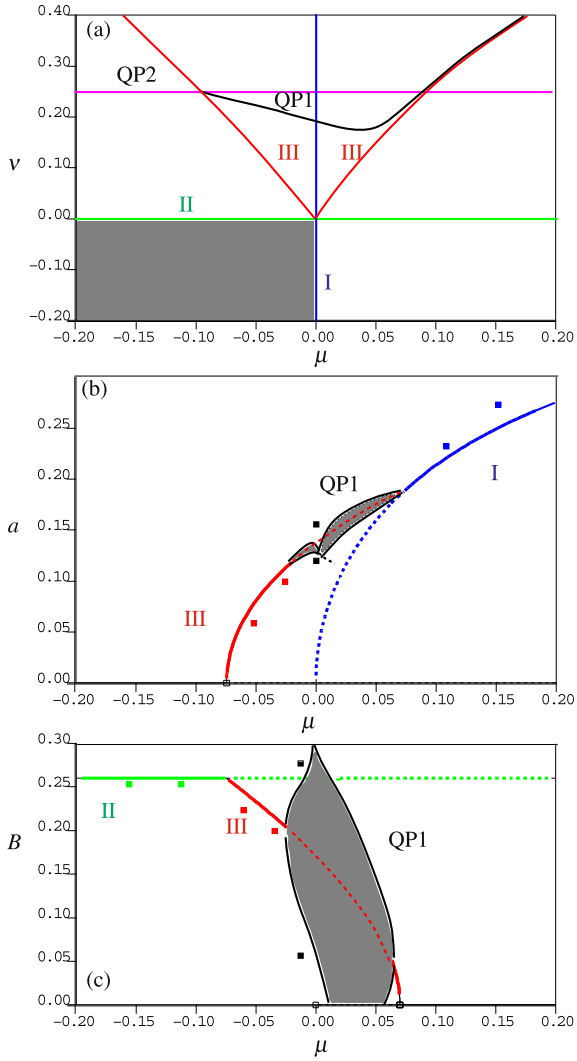

Fig. 4 Bifurcation diagrams when $\xi = -0.1$; (**a**) bifurcation loci on the (μ, ν)-plane; (**b**, **c**): amplitudes a and B vs. μ when $\xi = -0.1$ and $\nu = 0.2$. *Continuous line*: stable; *dashed line*: unstable; *boxes*: direct integrations

A larger damping, $\xi = -0.1$, is considered now, and relevant results displayed in Fig. 4. When the boundaries in Fig. 4a are compared with those in Fig. 3a, it results that the limits of existence of the solutions I, II, and III are unchanged, while the quasi-periodic solutions QP1 and QP2 are triggered for higher values of ν, and QP3 disappears. The plots of a and B vs. μ when $\nu = 0.2$ and $\xi = -0.1$ are shown in Fig. 4b and 4c. It appears that the quasi-periodic solution QP1 significantly interacts with the periodic and equilibrium solutions only at $\nu = 0.2$. A periodic orbit in the phase space $(a, B, \dot{B})$, corresponding to

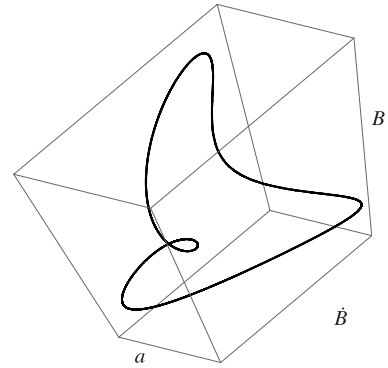

Fig. 5 Periodic orbit in $(a, B, \dot{B})$ corresponding to the quasi-periodic motion QP1 in (x, y), when $\xi = -0.1$, $\mu = 0.05$, $\nu = 0.2$

the quasi-periodic motion (in x, y) QP1, is shown in Fig. 5.

Time-series of a, B and the relevant reconstituted time evolutions of x, y are shown in Figs. 6 and 7, respectively, for $\mu = 0.04$, $\nu = 0.2, \xi = -0.1$, where a solution of QP1 kind is picked up. The latter plots are in good agreement with the corresponding time-series of x, y, as obtained from numerical integrations of the starting Eqs. (3), shown in Fig. 8.

The previous results show that the larger is $|\xi|$, the weaker is the interaction among periodic and quasiperiodic solutions. Indeed, when $|\xi|$ increases, the region of existence of QP1 moves to larger values of ν. When the system is far enough from the *DZH*-bifurcation, e.g., when $\xi = -0.8$ (Fig. 9), the quasiperiodic solutions are far from the origin of the (μ, ν)-plane (Fig. 9a), this entailing the almost total lack of interaction of quasiperiodic motions with periodic motions or equilibria. Consistently, bifurcation diagrams in Figs. 9b and 9c, relevant to $\nu = 0.1$ and $\xi = -0.8$, include just equilibria (II) and periodic solutions (I, III).

It is worth noticing that when the transition has been exhausted, Eqs. (27) provide results qualitatively consistent with those furnished by Eqs. (21a) and (21b). A comparison between boundaries obtained by Eqs. (27) (continuous lines) and Eqs. (21a) and (21b) (dashed lines) can be detected in Fig. 9a.

6 Concluding remarks

In this paper, the bifurcation equations for a two degrees-of-freedom mechanical system, exhibiting

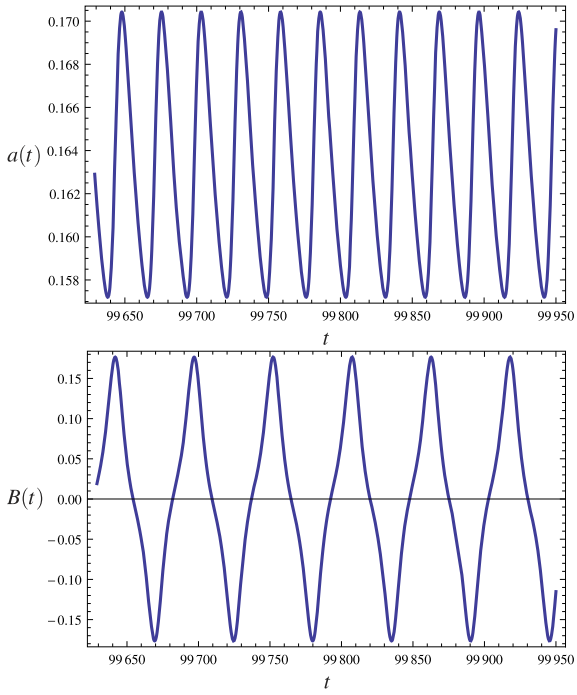

Fig. 6 Time evolution of a and B, corresponding to the quasiperiodic motion QP1 in (x, y), when $\xi = -0.1$, $\mu = 0.04$, $\nu = 0.2$

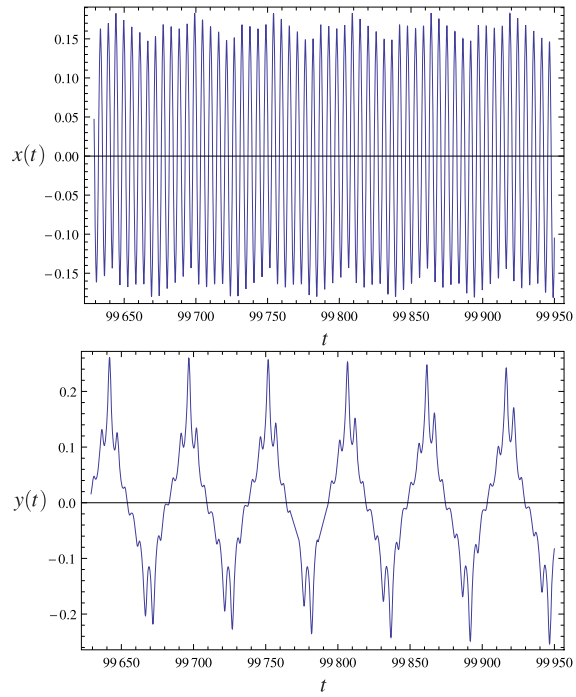

Fig. 7 Time evolution of x and y, reconstituted from MSM, describing the quasiperiodic motion QP1, when $\xi = -0.1$, $\mu = 0.04$, $\nu = 0.2$

double-zero/Hopf bifurcation (*DZH*), have been obtained by an enhanced version of the Multiple Scale Method (MSM). The equations are believed to be new in literature.

The implemented perturbation algorithm exhibits remarkable differences with respect to standard applications of the MSM, namely:

1. Fractional power expansions, both for the state variables and time scales, are adopted, due to the presence of a not-semisimple double zero eigenvalue (nil-potent Jordan block), although the purely imaginary eigenvalues are nondefective.
2. Arbitrary amplitudes appearing in the complementary part of the solution of the perturbation equations (and usually neglected in standard applications, or used for mere normalization purposes), cannot all be omitted here, since this would lead to inconsistent results, and loss of some terms in the bifurcation equations. Among all the amplitudes, it has been checked that just one (namely A_1) is essential; it describes a smaller but faster correction of the oscillation triggered by the Hopf bifurcation.
3. The reconstitution procedure, aimed to bring back the solvability conditions in a unique set of differential equations in the true time t, is not straightforward, as in standard cases. It could require the use of the Schwarz conditions, or, alternatively, ad hoc combinations of the solvability conditions, in order to achieve the goal.
4. A system of a first-order complex equation (as in the Hopf bifurcation) and a second-order real equation (as in the double-zero bifurcation), is found, however, coupled by mixed terms. As a result, a 4-dimensional dynamical system, governing the slow flow on the center manifold, is obtained. Finally, it is reduced to a 3-dimensional system (ϑ is a slave variable), coherently with the codimension of the problem.

Attentions has been focused on the transition between the codimension-3 *DZH*-bifurcation and the codimension-2 Zero/Hopf (*ZH*) bifurcation, when a bifurcation parameter (namely the damping of the subsystem undergoing the double zero eigenvalue), is increased in modulus. It has been shown that, in this limit process, the dynamics of the real amplitude become slower, thus justifying the lowering of the order of the differential equations, which tend to the 3-

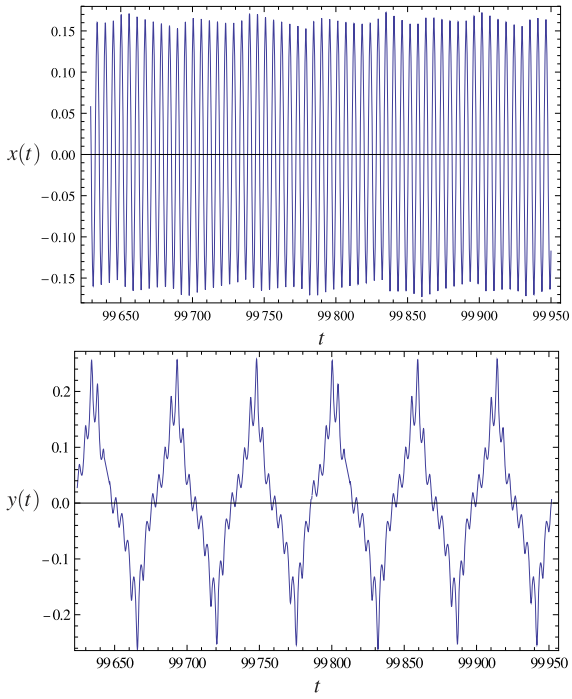

Fig. 8 Time evolution of x and y, obtained by numerical integrations of Eqs. (3a) and (3b), when $\xi = -0.1$, $\mu = 0.04$, $\nu = 0.2$

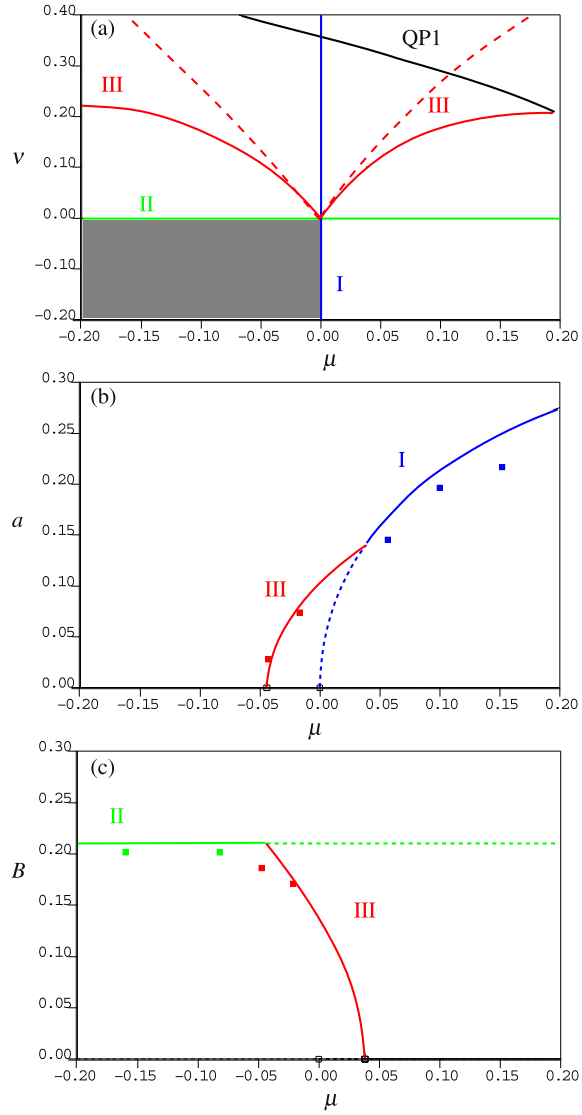

Fig. 9 Bifurcation diagrams when $\xi = -0.8$; (**a**) bifurcation loci on the (μ, ν)-plane, obtained by Eq. (27) (*continuous lines*) or Eqs. (21a) and (21b) (*dashed lines*); (**b**, **c**): amplitudes a and B vs. μ when $\xi = -0.8$ and $\nu = 0.1$ (*continuous line*: stable; *dashed line*: unstable; *boxes*: direct integrations)

dimensional equations governing the *ZH*-bifurcation. Therefore, the *DZH*-bifurcation equations are able to describe the transient regime. In contrast, bifurcation equations for *ZH* lose validity when damping becomes vanishingly small, since this appears as a small divisor in the equations. Numerical results highlighted the role of quasi-periodic solutions: they strongly affect the dynamics close to the codimension-3 bifurcation, but move away when the system approaches the codimension-2 bifurcation, thus explaining the transition mechanism.

Appendix A: Reconstitution procedure

The solvability conditions Eqs. (13), (15a), (15b), (17a), (17b), (18) must be substituted in Eq. (20a), (20b) to get the reconstituted equations (21a) and (21b). During the reconstitution procedure, the key-term $\alpha_5(d_2^2 A_0 + 2d_1 d_2 A_1)$, occurring in the equation related to the amplitude A, has to be written as $\alpha_5(d_1(d_2 A_1) + d_2(d_1 A_1 + d_2 A_0))$, requiring t_1-differentiation of Eq. (17a) and t_2-differentiation of Eq. (15a). As a consequence, second and third derivatives of the amplitudes occur, which can be easily evaluated by differentiating Eq. (15a). In this case, no problems in the reconstitution procedure would occur.

If, in contrast, other procedures were followed (e.g., $d_2^2 A_0$ evaluated by t_2-differentiation of Eq. (15a) and $2d_1 d_2 A_1$ by t_1-differentiation of Eq. (17a) or by t_2-differentiation of Eq. (15a)), some inconsistency would appear that could be overcome only by using

the Schwarz condition

$$d_1(d_2A_1) = d_2(d_1A_1). \tag{28}$$

An alternative way to handle the reconstitution procedure is to separately zeroing terms depending on t_1 and terms not depending on it, thus causing a splitting of the solvability conditions. In particular, from Eq. (15a) it follows:

$$d_2A_0 = \alpha_1 A_0 + \alpha_3 A_0^2 \bar{A}_0, \tag{29a}$$

$$d_1A_1 = \alpha_2 A_0 B_0^2 \tag{29b}$$

and from Eq. (17a)

$$d_3A_0 = 0, \tag{30a}$$

$$\begin{aligned} d_2A_1 = {} & \alpha_1 A_1 + \alpha_2 A_1 B_0^2 + \alpha_3\big(2A_0\bar{A}_0A_1 + A_0^2\bar{A}_1\big) \\ & + \alpha_4 A_0 B_0 d_1 B_0 + \alpha_5 d_1^2 A_1. \end{aligned} \tag{30b}$$

Now, in the key-term $\alpha_5(d_2^2A_0 + 2d_1d_2A_1)$, $d_2^2A_0$ can be evaluated by differentiation of Eq. (29a) and the remaining $2d_1d_2A_1$ either by t_2-differentiation of (29b) or by t_1-differentiation of (30b). Of course, the two choices would entail inconsistencies in the reconstitution, if the Schwarz condition $d_1(d_2A_1) = d_2(d_1A_1)$ were not explicitly enforced. Again, the latter solves the problem.

Appendix B: Coefficients of the equations

The coefficients of Eq. (9) are

$$\begin{aligned} &\mathcal{F}_2(x_0, y_0, x_1) \\ &\quad = -2d_0d_1x_1 - 2d_0d_2x_0 - d_1^2x_0 + \mu d_0x_0 \\ &\qquad + \xi_{01}(d_0y_0 - d_0x_0) + \kappa_{01}(y_0 - x_0) \\ &\qquad + \xi_{03}(d_0y_0 - d_0x_0)(y_0 - x_0)^2 \\ &\qquad + \kappa_{03}(y_0 - x_0)^3 - \xi_{13}d_0x_0x_0^2 \\ &\qquad - \kappa_{13}x_0^3, \end{aligned} \tag{31}$$

$$\begin{aligned} &\mathcal{G}_2(x_0, y_0, y_1) \\ &\quad = -2d_0d_1y_1 - 2d_0d_2y_0 - d_1^2y_0 + \xi d_0y_0 \\ &\qquad + \nu y_0 - \alpha\xi_{01}(d_0y_0 - d_0x_0) \\ &\qquad - \alpha\kappa_{01}(y_0 - x_0) - \alpha\kappa_{03}(y_0 - x_0)^3 \\ &\qquad - \alpha\xi_{03}(d_0y_0 - d_0x_0)(y_0 - x_0)^2 \\ &\qquad - \xi_{23}d_0y_0y_0^2 - \kappa_{23}y_0^3. \end{aligned}$$

The coefficients of Eq. (10) are

$$\begin{aligned} &\mathcal{F}_3(x_0, y_0, x_1, y_1, x_2) \\ &\quad = -2d_0d_1x_2 - 2d_0d_2x_1 - 2d_1d_2x_0 \\ &\qquad - 2d_0d_3x_0 - d_1^2x_1 + \mu(d_0x_1 + d_1x_0) \\ &\qquad + \kappa_{01}(y_1 - x_1) - 3\kappa_{13}x_1x_0^2 \\ &\qquad + \xi_{01}(d_1y_0 - d_1x_0 + d_0y_1 - d_0x_1) \\ &\qquad + \xi_{03}(d_1y_0 - d_1x_0 + d_0y_1 - d_0x_1)(y_0 - x_0)^2 \\ &\qquad + 2\xi_{03}(d_0y_0 - d_0x_0)(y_0 - x_0)(y_1 - x_1) \\ &\qquad + 3\kappa_{03}(y_1 - x_1)(y_0 - x_0)^2 \\ &\qquad - \xi_{13}(d_0x_1 + d_1x_0)x_0^2 - 2\xi_{13}d_0x_0x_1x_0, \\ &\mathcal{G}_3(x_0, y_0, x_1, y_1, y_2) \\ &\quad = -2d_0d_1y_2 - 2d_0d_2y_1 - 2d_1d_2y_0 \\ &\qquad - 2d_0d_3y_0 - d_1^2y_1 + \xi(d_0y_1 + d_1y_0) \\ &\qquad + \nu y_1 - \alpha\kappa_{01}(y_1 - x_1) - 3\kappa_{23}y_1y_0^2 \\ &\qquad - \alpha\xi_{01}(d_1y_0 - d_1x_0 + d_0y_1 - d_0x_1) \\ &\qquad - \alpha\xi_{03}(d_1y_0 - d_1x_0 + d_0y_1 - d_0x_1)(y_0 - x_0)^2 \\ &\qquad - 2\alpha\xi_{03}(d_0y_0 - d_0x_0)(y_0 - x_0)(y_1 - x_1) \\ &\qquad - 3\alpha\kappa_{03}(y_1 - x_1)(y_0 - x_0)^2 \\ &\qquad - \xi_{23}(d_0y_1 + d_1y_0)y_0^2 - 2\xi_{23}d_0y_0y_1y_0. \end{aligned} \tag{32}$$

The coefficients of Eqs. (15a), (15b), (17a), (17b) and (18) are

$$\alpha_1 = (\mu + i\kappa_{01} - \xi_{01})\frac{1}{2},$$

$$\alpha_2 = (3i\kappa_{03} - \xi_{03})\frac{1}{2},$$

$$\alpha_3 = (3i\kappa_{03} + 3i\kappa_{13} - \xi_{03} - \xi_{13})\frac{1}{2},$$

$$\alpha_4 = i\xi_{03},$$

$$\alpha_5 = \frac{i}{2},$$

$$\alpha_6 = (\xi_{01} - \mu)\frac{i}{2},$$

$$\alpha_7 = (\xi_{03} + \xi_{13})\frac{i}{2},$$

$$\alpha_8 = \frac{i\xi_{03}}{2},$$

$$
\begin{aligned}
\alpha_9 &= -\alpha\kappa_{01}\xi_{01} + \alpha\left(\kappa_{01}^2 - \xi_{01}^2\right)\frac{i}{2},\\
\alpha_{10} &= (1-\alpha)(\kappa_{01}\xi_{03} - 3i\kappa_{01}\kappa_{03}) - 3\alpha\kappa_{03}\xi_{01}\\
&\quad - i\alpha\xi_{01}\xi_{03},\\
\alpha_{11} &= -3\alpha\kappa_{03}\xi_{01} - 2\alpha\kappa_{01}\xi_{03}\\
&\quad + i(6\alpha\kappa_{01}\kappa_{03} - \alpha\xi_{01}\xi_{03}),\\
\beta_1 &= \nu - \alpha\kappa_{01},\\
\beta_2 &= -(\alpha\kappa_{03} + \kappa_{23}),\\
\beta_3 &= -6\alpha\kappa_{03},\\
\beta_4 &= \xi - \alpha\xi_{01},\\
\beta_5 &= -(\alpha\xi_{03} + \xi_{23}),\\
\beta_6 &= -2\alpha\xi_{03},\\
\beta_7 &= -2\alpha\xi_{03},\\
\beta_8 &= \alpha\kappa_{01}^2,\\
\beta_9 &= 4\alpha\kappa_{01}\kappa_{03},\\
\beta_{10} &= 12\alpha\kappa_{01}\kappa_{03}(1-\alpha)
\end{aligned}
\tag{33}
$$

and the coefficients of Eqs. (21a), (21b) and (22a), (22b) are

$$
\begin{aligned}
\eta_1 &= -\frac{\xi_{01}}{2} - \alpha\kappa_{01}\xi_{01},\\
\eta_2 &= \frac{1}{2},\\
\eta_3 &= 0,\\
\eta_4 &= \frac{1}{4}(3\kappa_{03} + \kappa_{01})\xi_{03} - 3\alpha\kappa_{03}\xi_{01} - \frac{\xi_{03}}{2}\\
&\quad + \frac{3\kappa_{13}\xi_{01}}{4} - 2\alpha\kappa_{01}\xi_{03},\\
\eta_5 &= -\frac{3}{4}(\kappa_{03} + \kappa_{13}),\\
\eta_6 &= -\frac{\xi_{03}}{4},\\
\eta_7 &= -\frac{3\kappa_{03}}{2},\\
\eta_8 &= -\frac{\xi_{03}}{2} - 3\alpha\kappa_{03}\xi_{01} + \left(1 - \frac{7}{8}\alpha\right)\kappa_{01}\xi_{03},\\
\eta_9 &= -\frac{\xi_{03}}{8},\\
\eta_{10} &= 0,\\
\eta_{11} &= -\alpha\xi_{01},\\
\eta_{12} &= -2\alpha\xi_{03},\\
\eta_{13} &= -(\alpha\xi_{03} + \xi_{23}),\\
\eta_{14} &= -\alpha\kappa_{01}(1 - \kappa_{01}),\\
\eta_{15} &= -6\alpha\kappa_{03} + 12\alpha\kappa_{01}\kappa_{03}(1-\alpha) + 2\alpha\xi_{01}\xi_{03},\\
\eta_{16} &= -2\alpha\xi_{03},\\
\eta_{17} &= -\alpha\kappa_{03} - \kappa_{23} + 4\alpha\kappa_{01}\kappa_{03}
\end{aligned}
\tag{34}
$$

and

$$
\begin{aligned}
\zeta_1 &= \frac{1}{2}\left[\kappa_{01} + \alpha\left(\kappa_{01}^2 - \xi_{01}^2\right) - \frac{1}{2}\left(\kappa_{01}^2 + \xi_{01}^2\right)\right],\\
\zeta_2 &= \frac{\xi_{01}}{4},\\
\zeta_3 &= -\frac{1}{8},\\
\zeta_4 &= \frac{3}{2}(\kappa_{03} + \kappa_{13}) + \kappa_{01}\kappa_{03}\left(6\alpha - \frac{3}{4}\right) - \frac{3}{4}\kappa_{01}\kappa_{13}\\
&\quad - \frac{\xi_{01}}{4}(\xi_{03} + \xi_{13}) - \alpha\xi_{01}\xi_{03},\\
\zeta_5 &= \frac{1}{4}(\xi_{03} + \xi_{13}),\\
\zeta_6 &= -\frac{3}{4}\kappa_{03},\\
\zeta_7 &= \frac{\xi_{03}}{2},\\
\zeta_8 &= \frac{3}{2}\kappa_{03} + \kappa_{01}\kappa_{03}\left(\frac{27}{8}\alpha - \frac{15}{4}\right) - \left(\alpha + \frac{1}{4}\right)\xi_{01}\xi_{03},\\
\zeta_9 &= -\frac{3}{8}\kappa_{03},\\
\zeta_{10} &= \frac{\xi_{03}}{4}.
\end{aligned}
\tag{35}
$$

References

1. Guckenheimer, J., Holmes, P.: Nonlinear Oscillations, Dynamical Systems, and Bifurcation of Vector Fields. Springer, New York (1983)
2. Luongo, A., Paolone, A.: Multiple scale analysis for divergence-Hopf bifurcation of imperfect symmetric systems. J. Sound Vib. **218**, 527–539 (1998)
3. Augusti, G.: Instability of struts subject to radiant heat. Meccanica **3**, 167–176 (1968). http://dx.doi.org/10.1007/BF02129249.10.1007/BF02129249
4. Holmes, P.J.: Bifurcations to divergence and flutter in flow-induced oscillations: a finite dimensional analysis. J. Sound Vib. **53**, 471–503 (1977)

5. Troger, H., Steindl, A.: Nonlinear Stability and Bifurcation Theory. An Introduction for Engineers and Applied Scientists. Springer, Wien (1991)
6. Elishakoff, I., Lottati, I.: Divergence and flutter of nonconservative systems with intermediate support. Comput. Methods Appl. Mech. Eng. **66**(2), 241–250 (1988)
7. Impollonia, N., Elishakoff, I.: Effect of elastic foundations on divergence and flutter of an articulated pipe conveying fluid. J. Fluids Struct. **14**, 559–573 (2000)
8. Tondl, A.: Determination of the limit of initiation of self-excited vibration of rotors. Int. J. Non-Linear Mech. **15**, 417–428 (1980)
9. Rega, G., Alaggio, R.: Experimental unfolding of the nonlinear dynamics of a cable-mass suspended system around a divergence-Hopf bifurcation. J. Sound Vib. **322**, 581–611 (2009)
10. Jayaraman, G., Struthers, A.: Divergence and flutter instability of elastic specially orthotropic plates subject to follower forces. J. Sound Vib. **281**, 357–373 (2005)
11. Fazelzadeh, S.A., Marzocca, P., Mazidi, A., Rashidi, E.: Divergence and flutter of shear deformable aircraft swept wings subjected to roll angular velocity. Acta Mech. **212**, 151–165 (2010)
12. Bigoni, D., Noselli, G.: Experimental evidence of flutter and divergence instabilities induced by dry friction. J. Mech. Phys. Solids **59**, 2208–2226 (2011)
13. Tomski, L., Uzny, S.: The regions of flutter and divergence instability of a column subjected to beck's generalized load, taking into account the torsional flexibility of the loaded end of the column. Mech. Res. Commun. **38**, 95–100 (2011)
14. Peterka, F.: Bifurcations and transition phenomena in an impact oscillator. Chaos Solitons Fractals **7**, 1635–1647 (1996)
15. Wieczorek, S., Simpson, T.B., Krauskopf, B., Lenstra, D.: Bifurcation transitions in an optically injected diode laser: theory and experiment. Opt. Commun. **215**, 125–134 (2003)
16. Kuehn, C.: A mathematical framework for critical transitions: Bifurcations, fast-slow systems and stochastic dynamics. Physica D, Nonlinear Phenom. **240**, 1020–1035 (2011)
17. Nayfeh, A.H., Mook, D.T.: Nonlinear Oscillations. Wiley, New York (1979)
18. Luongo, A., Di Egidio, A., Paolone, A.: Multiple-timescale analysis for bifurcation from a multiple-zero eigenvalue. AIAA J. **41**(6), 1143–1150 (2003)
19. Luongo, A., Di Egidio, A., Paolone, A.: Multiple scale bifurcation analysis for finite-dimensional autonomous systems. In: Recent Research Developments in Sound & Vibrations, pp. 161–201. Transworld Research Network, Kerdala, India (2002)
20. Arkhipova, I.M., Luongo, A., Seyranian, A.P.: Vibrational stabilization of the upright statically unstable position of a double pendulum. J. Sound Vib. **331**(2), 457–469 (2012)
21. Luongo, A., Zulli, D.: The multiple scales method for the analysis of a double-zero/single-Hopf bifurcation. In: XX AIMETA Conference—Italian Association of Theoretical and Applied Mechanics. Bologna, Italy, September 2011 (2011). http://www.lamc.ing.unibo.it/aimeta2011/
22. Rand, R.H., Holmes, P.J.: Bifurcation of periodic motions in two weakly coupled Van der Pol oscillators. Int. J. Non-Linear Mech. **15**, 387–399 (1980)
23. Storti, D.W., Rand, R.H.: Dynamics of two strongly coupled Van der Pol oscillators. Int. J. Non-Linear Mech. **17**, 143–152 (1982)
24. Chakraborty, T., Rand, R.H.: The transition from phase locking to drift in a system of two weakly coupled Van der Pol oscillators. Int. J. Non-Linear Mech. **23**, 369–376 (1988)
25. Rajasekar, S., Murali, K.: Resonance behaviour and jump phenomenon in a two coupled Duffing–Van der Pol oscillators. Chaos Solitons Fractals **19**, 925–934 (2004)
26. Bi, Q.: Dynamical analysis of two coupled parametrically excited Van der Pol oscillators. Int. J. Non-Linear Mech. **39**, 33–54 (2004)
27. Kuznetsov, A.P., Roman, J.P.: Properties of synchronization in the systems of non-identical coupled Van der Pol and Van der Pol–Duffing oscillators. Broadband synchronization. Physica D, Nonlinear Phenom. **238**, 1499–1506 (2009)
28. Kuznetsov, A.P., Stankevich, N.V., Turukina, L.V.: Coupled Van der Pol–Duffing oscillators: phase dynamics and structure of synchronization tongues. Physica D, Nonlinear Phenom. **238**, 1203–1215 (2009)
29. Vakakis, A.F., Gendelman, O.V., Bergman, L.A., McFarland, D.M., Kerschen, G., Lee, Y.S.: Nonlinear Targeted Energy Transfer in Mechanical and Structural Systems. Springer, New York (2008)
30. Seyranian, A.P., Mailybaev, A.A.: Multiparameter Stability Theory with Mechanical Applications. World Scientific, New Jersey (2003)
31. Luongo, A.: Eigensolutions sensitivity for nonsymmetric matrices with repeated eigenvalues. AIAA J. **317**(7), 1321–1328 (1993)
32. Luongo, A., Di Egidio, A.: Divergence, Hopf and double-zero bifurcations of a nonlinear planar beam. Comput. Struct. **84**, 1596–1605 (2006)
33. Luongo, A., Di Egidio, A., Paolone, A.: Multiscale analysis of defective multiple-Hopf bifurcations. Comput. Struct. **82**, 12705–12722 (2004)
34. Dankowicz, H., Lacarbonara, W.: On various representations of higher order approximations of the free oscillatory response of nonlinear dynamical systems. J. Sound Vib. **330**, 3410–3423 (2011)
35. Doedel, E.J.: AUTO-07P: Continuation and Bifurcation Software for Ordinary Differential Equation (2007). http://sourceforge.net/projects/auto-07p/